Manufacturing and Performance Evaluation of a Refractive Real-Time MWIR Hyperspectral Imager

Brian Catanzaro[a], Mark Dombrowski[b], Paul Willson[c], Jeff Hendrixson[d], Eric Hillenbrand[d], John Wilcox[e]

[a] CFE Services, 5147 Pacifica Dr., San Diego, CA 92109[1]
[b] Surface Optics Corporation
[c] Picatinny Arsenal
[d] Naval Surface Warfare Center, Crane Division
[e] Wilcox Engineering

ABSTRACT

Hyperspectral imaging in the 2-5 um band has held interest for applications in detection and discrimination of targets. Real time instrumentation is particularly powerful as a tool for characterization and field measurement. A compact, real-time, refractive MWIR hyperspectral imaging instrument has been designed and is undergoing testing. Using a combination of dispersive and corrective elements, the system has been designed for integration and preliminary test at room temperature with passive focus correction for the cryogenic elements. The F/1.75 design supports near diffraction limited performance from 2.5 um to 5.0 um. This paper will review the challenges in manufacturing such a system as well as the alignment and performance data.

Keywords: Hyperspectral imaging, MWIR, ZnSe, Cryogenic, Microbolometer

1. REAL-TIME HYPERSPECTRAL IMAGING

Real-time imaging over broad bands in the electromagnetic spectrum from the ultraviolet (UV) through the infrared (IR) has been a staple in the areas of remote sensing, surveillance, target detection and tracking, search and homing devices, spectrally tailored coating development, nondestructive inspection, and noninvasive diagnosis. Improvements are being made in these techniques all the time, with increased resolution, higher sensitivity, and greater information throughput being the benefit. Instrumentation developed at Surface Optics has been used to distinguish objects based on their spectral signature in a number of applications. These include: revealing camouflaged military targets, friend-foe identification based on subtle coloring of personnel uniforms, and tracking of civilian vehicles based on spectral signature. [1,2]

In order to address some of the demands of the hyperspectral imaging community, a real-time hyperspectral imager for the mid-wave infrared (MWIR) is under development at Surface Optics. The goals for the hyperspectral imager are:

- Real-time hyperspectral output
- Waveband that spans from 2 μm to 5 μm
- High signal to noise ratio
- Long lifetime for coolant (+12 hrs)
- Room temperature and cooled operation
- Field portable

The design incorporates an achromatic optical system that spans the required wavelength band. A proprietary scanning technique along with custom image processing electronics is designed to provide real-time hyperspectral information. A high signal to noise (SNR) is achieved by cooling the majority of the optical system to cryogenic temperature. Long

[1] Correspondence - Email: bcatanza@alumni.caltech.edu; Telephone: 858-204-6299

Infrared Technology and Applications XXIX, Bjørn F. Andresen, Gabor F. Fulop, Editors,
Proceedings of SPIE Vol. 5074 (2003) © 2003 SPIE · 0277-786X/03/$15.00

lifetime for the coolant is achieved by an efficient dewar and the low thermal mass contributed to a rapid cool down. The optical system has been designed to image with the optics at both room temperature and cryogenic temperature. Finally, the unit has been designed to minimize the mass and the footprint in order to allow it to be field portable.

The optical, thermal, and mechanical design for the MWIR hyperspectral imager (MWIR HSI) has been completed. At this stage, the optical system is being assembled and tested in sub-assemblies prior to final integration and test. This paper will describe the optical and mechanical design of the MWIR HSI. The opto-mechanical tolerancing will be discussed. Issues specific to designing the system for cryogenic operation will be outlined and the approach for addressing them will be reviewed. Finally, initial resolution testing of the lenses at both room temperature and cryogenic temperature will be presented.

2. OPTICAL DESIGN FOR THE MWIR HSI

In order to meet the unique requirements for this system, several architectures were studied. These include refractive, refractive-reflective, all-reflective optical systems. Moving and stationary filters were also explored. Finally, an all refractive design was selected that incorporates a proprietary scanning mechanism to achieve the goals for real-time hyperspectral imaging.

The design uses three infinite conjugates to provide images from targets at distances greater than 5 m. Two of the infinite conjugates are arranged as a telecentric imaging system. A refractive prism assembly provides the dispersion necessary to distinguish the wavebands. The prism assemblies and multi-element infinite conjugates provide both achromatic performance as well as functionality at both room temperature and after cooling the optics to cryogenic temperature.

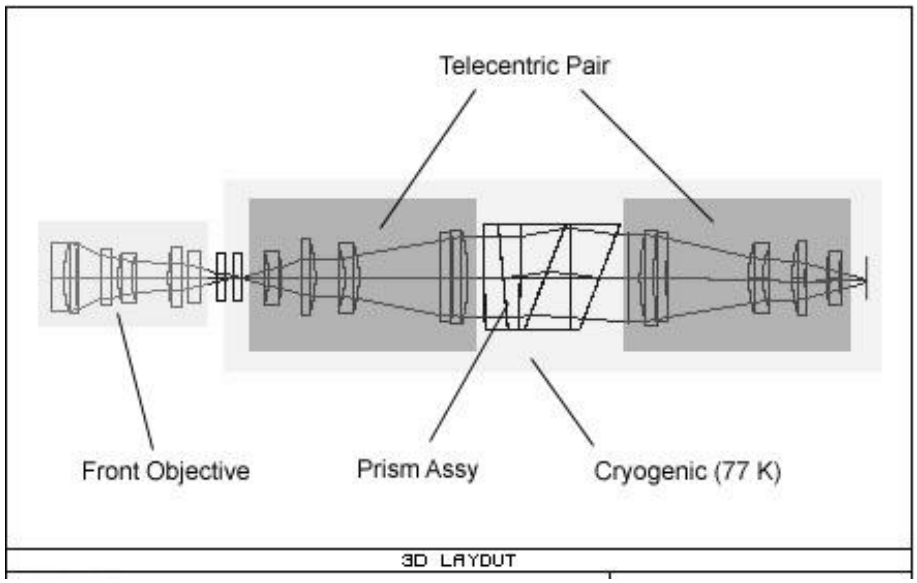

Figure 1: Raytrace of MWIR HSI

Figure 1 shows the layout of the optical system. The system is F/1.75 with a focal length of 50 mm. The optical model contains material properties for strain of the housing and optical materials as well as the index changes for operation at cryogenic temperature. The performance is near diffraction limit for both the room temperature and cryogenic temperature. Figure 2 shows the wavefront error at cryogenic temperature over the waveband. Figure 3 shows a comparison of the spot diagram at both room temperature and cryogenic temperature for $\lambda = 3$ μm. Note that the spot diameter is very close to the Airy diameter for cryogenic temperature and within a factor of two of the Airy diameter for room temperature.

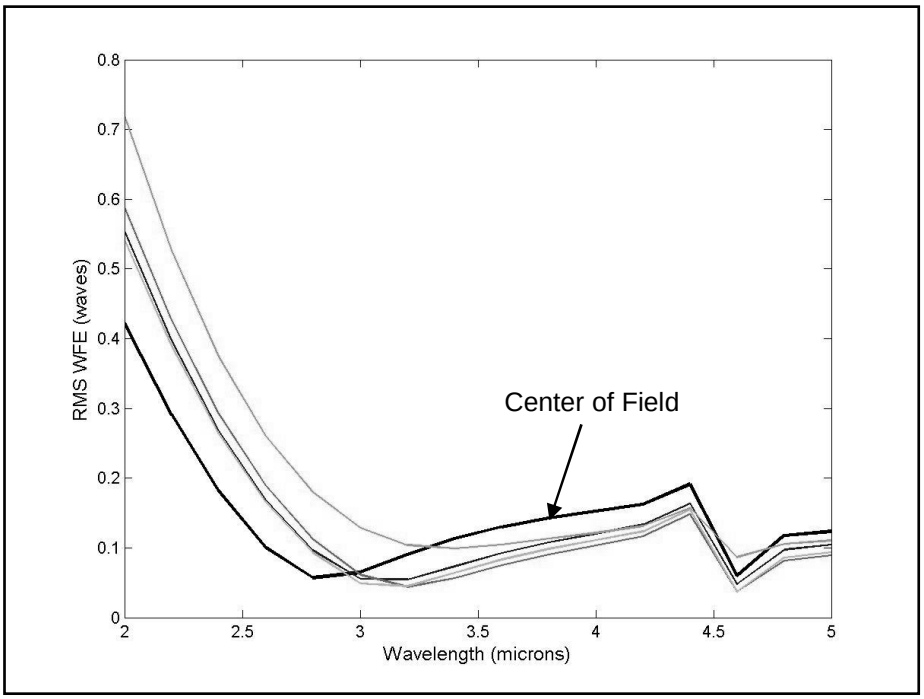

Figure 2: RMS Wavefront Error over the Spectral Range of the Instrument

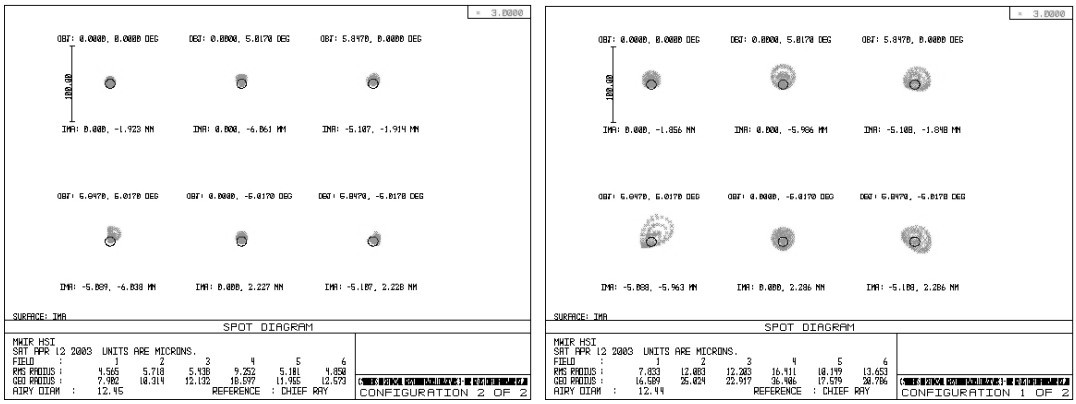

Figure 3: Spot Diagram for Cyrogenic (left) and Room Temperature (right)

The mechanical configuration for this optical system is shown in Figure 4. The system incorporates a compact dewar and a scanning mirror and calibration shutter assembly. The overall length of the system is less than 0.6 m.

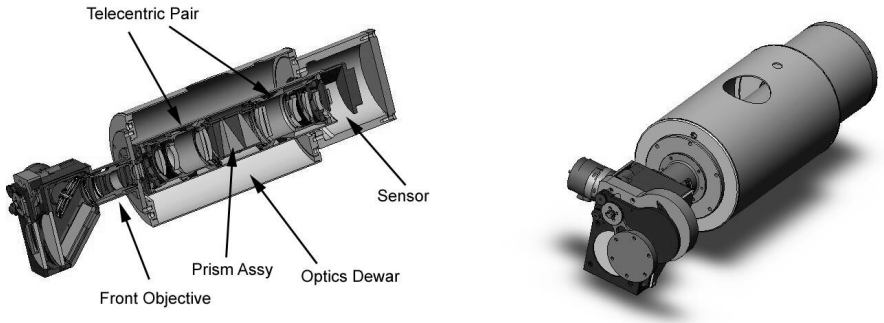

Figure 4: Mechanical Layout of MWIR HSI

3. OPTO-MECHANICAL TOLERANCING

The sensitivity of performance to opto-mechanical manufacturing errors often increases dramatically with the speed of the system. In order to establish the tolerances for manufacturing and assembly, the sensitivity of the performance with respect to errors was evaluated. The performance of the MWIR HSI can be evaluated in a very complex fashion including MTF performance over the field of view as well as over the waveband. However, for computational efficiency the RMS wavefront error (WFE) at a single wavelength (λ = 3 μm) was used to establish sensitivity and tolerance.

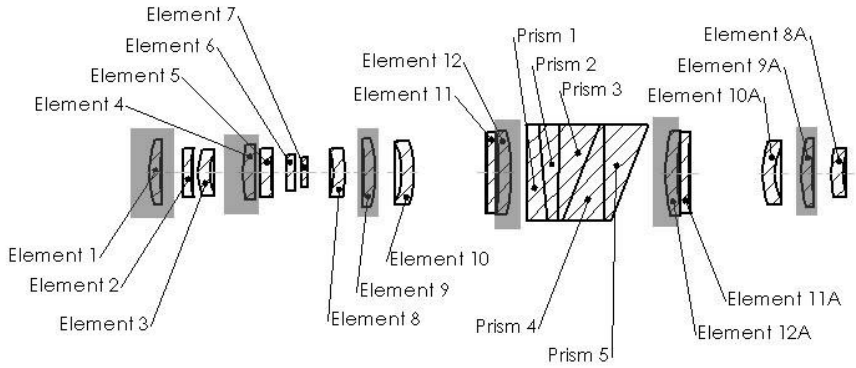

Figure 5: Performance of the System was Most Sensitive to the *Highlighted* Elements

Upon evaluating the sensitivity of RMS WFE to decenter and despace errors, certain elements were identified as critically placed components. The tolerance was then set to ±25 μm for decenter and ±12 μm for despace as a result of the sensitivity of these critical elements. A Monte Carlo simulation was then computed using these tolerances for all of the elements. The results of these statistics are shown in Figure 6. This indicates that the overwhelming number of scenarios result in less than 8.5 μm increase in the RMS radial spot size.

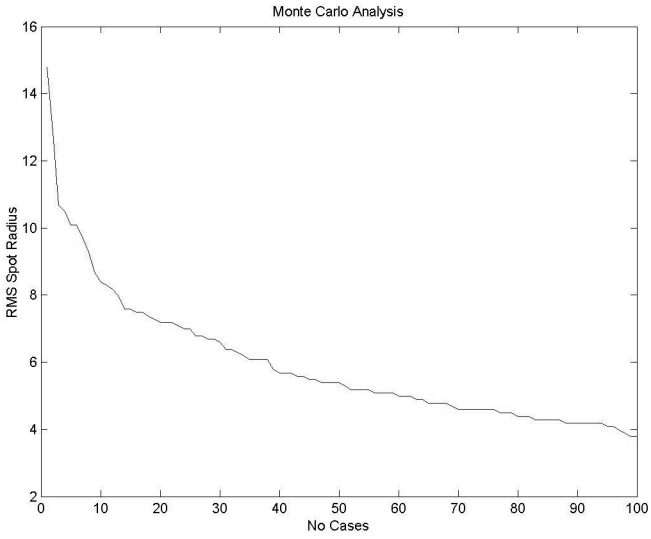

Figure 6: Tolerancing Indicates an Increase of RMS Spot Radius < 8.5 μm for 90% of the Cases

4. CRYOGENIC DESIGN ISSUES

Operating the MWIR HSI at cryogenic temperature results in a number of challenges. The most prominent of these are: focal length shift, stress in the optical elements, and coating survivability.

The focal length shift is critical for this telecentric imaging system. Using material properties for the cryogenic strain for the optics and the housing as well as the index change, the front focal length (FFL)/back focal length (BFL) of the system were calculated:

- BFL at Room Temperature 11.798 mm
- BFL at Cryogenic Temperature 11.964 mm

In particular, the material properties for the housing were verified using a mirror mounted in a dewar and a laser triangular sensor. The measurement demonstrated an error of less than 10% from values from the literature.

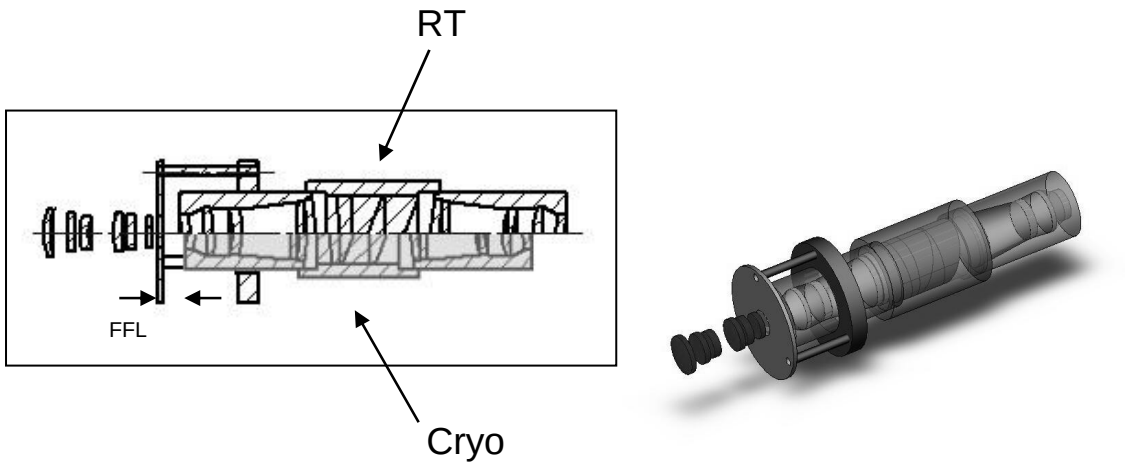

Figure 7: Actuator Designed from Invar/Aluminum to Correct for Focal Length Changes as a Result of Operation at Cryogenic Temperature

The BFL is longer at cold temperature. As such, an athermalizing actuator was designed using invar struts mounted to the aluminum housing. The reference point for the actuators was selected so that as the housing contracted, the focal plane moved away from the last element. Figure 7 shows the configuration for one half of the system. Using this approach, the system will be in focus at both room temperature and cryogenic temperature.

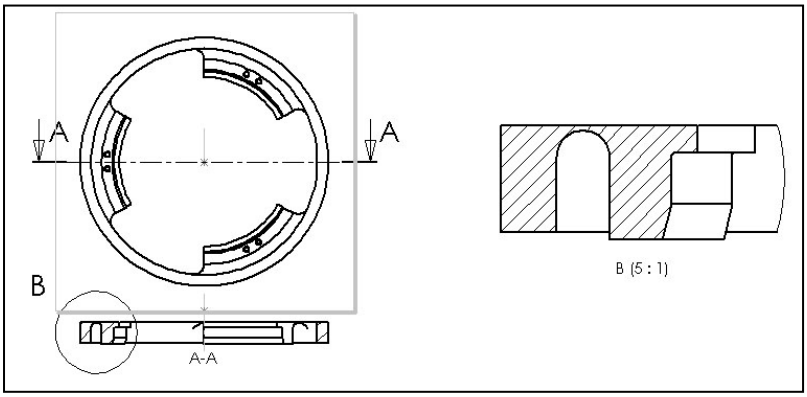

Figure 8: Flexure Design for Lens Cells

Differential strain from exposing the optical materials and the housing to cryogenic temperature can cause stress to the optical components. This can cause wavefront errors and/or fractures in the optical components. In order to relieve the stress, a simple flexure was designed (see Figure 8). A thin T-Shaped flexure tab was used to retain the optic in the mount. In order to size the flexure, an estimate of the stress was calculated based on analytical formulas and then an experiment was conducted to verify the effect on the optic.

If the flexure responds to the differential strain by bending, the stress will be related to the spring rate of the flexure and the displacement. The spring rate can be approximated by

$$\sigma = \frac{F}{A} = \frac{k_{bend}\delta L}{A_{contact}} = \frac{k_{bend}\Delta\varepsilon_{thermal}\rho_{lens}}{t_{lens} \times 2\pi\rho_{lens}/2} = \frac{k_{bend}\Delta\varepsilon_{thermal}}{\pi t_{lens}}$$

where σ is the stress on the perimeter of the optic, k_{bend} is the bending spring rate of the flexure, δL is the differential expansion of the lens and lens cell, $\Delta\varepsilon$ is the differential strain of the lens and lens cell, ρ_{lens} is the half the diameter of the lens, t_{lens} is the thickness of the contact area between the lens and lens cell. The bending stiffness of the flexure can be approximated as:

$$k_{bend} = \frac{3E_M I}{L^3} = \frac{3E_M\left(1/12 T^3 W\right)}{L^3} = \frac{E_M W}{4}\left(\frac{T}{L}\right)^3$$

where E_M is the modulus of elasticity of the flexure, I is the moment of inertia of the flexure, L is the length of the flexure, T is the thickness of the flexure, and W is the width of the flexure. The flexure for this lens cell is an annulus. As an estimate of stiffness, W is assumed to be the circumferential length. The actual flexure is anticipated to be stiffer than this approximation.

The final equation for stress is:

$$\sigma = \frac{k_{bend}\Delta\varepsilon_{thermal}}{\pi t_{lens}} \cong E_M\Delta\varepsilon_{thermal}\frac{1}{\pi t_{lens}} \times \frac{W}{4}\left(\frac{T}{L}\right)^3 = E_M\Delta\varepsilon_{thermal}\frac{\rho_{lens}}{4t_{lens}} \times \left(\frac{T}{L}\right)^3$$

Silicon is the worst case material for stress since the differential expansion between the lens cell housing and lens is the highest for all of the materials. Using the following values for the geometry of the lens cell, the stress is: 14 MPa (E_M = 70 GPa; ρ_{lens} = 15 mm; $\Delta\varepsilon_{thermal}$ = 3500 ppm; t_{lens} = 4 mm; T = 0.25 mm; L = 1 mm).

Radial stress in lens cells has been evaluated by Bayar [3] and reported in Yoder [4]:

$$\sigma = \frac{\Delta\varepsilon_{thermal}}{1/E_G + \left(\frac{\rho_{lens}}{h_{wall}}\right) 1/E_M}$$

where E_G is the modulus of elasticity of the lens material (131GPa for silicon), h_{wall} is thickness of the lens cell wall. Since the flexure is much more compliant than the lens cell wall, the lens cell wall can be ignored. Instead the spring rate of the flexure in radial compression can be used. The modified equation is:

$$\sigma = \frac{\Delta\varepsilon_{thermal}}{1/E_G + \left(\frac{\rho_{lens}}{L}\right)\left(\frac{t_{lens}}{W}\right) 1/E_M}.$$

For the geometry of the lens cell the stress is 6 MPa.

The stress can be converted to WFE using

$$W_{stress} = \left(\Delta n_{stress} \times \sigma\right) \times \left(\frac{t_{OPD}}{\lambda}\right)$$

where W_{stress} is the wavefront error in waves, Δn_{stress} is the stress optic coefficient, σ is the stress imparted to the optic, t_{OPD} is the thickness of the lens where it is under stress, and λ is the wavelength of operation. Typical values for stress optic coefficients for visible glasses are less than 3.0 x 10^{-6} mm^2/N (3.0 x 10^{-6} 1/Pa). One method of estimating the total stress is to combine the bending and radial stress using a root-summed-squared approach. In the example given, the combined stress is 15 MPa. Assuming that the stress is concentrated at the edge of the lens, t_{OPD} should be close to t_{lens} (4 mm). During operation, the worst wavefront error will occur at the shortest wavelength (λ = 2 μm). With these assumptions, the wavefront error is 0.093 λ P-V at the worst location.

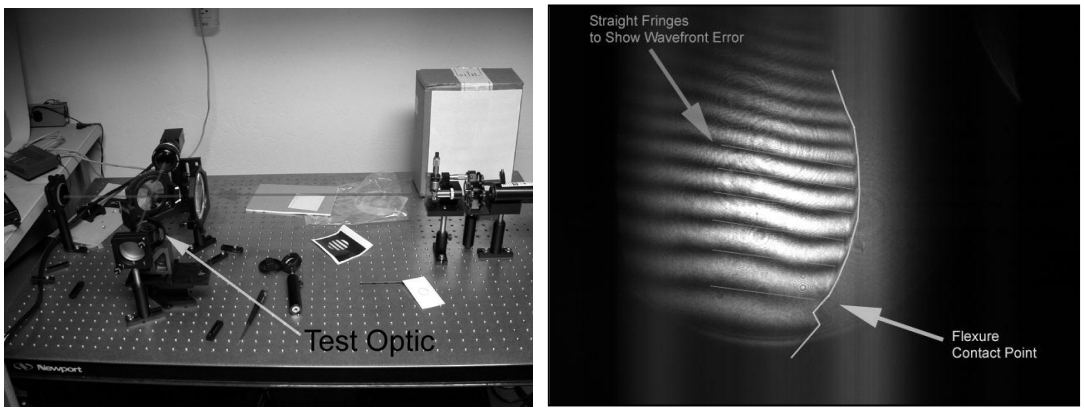

Figure 9: Interferometric Test of Stressed Optic (left) and Interfeogram at 0.6238 μm (right)

Rather than relying solely on this calculation, an experimental verification was performed. A sample ZnSe window was mounted in the lens cell. Shims of the appropriate thickness were used to simulate the stress on the optic. The window

was placed into a Michelson interferometer and the wavefront error was evaluated. Figure 9 shows the wavefront error in the proximity of the flexure. The peak to valley error was approximately 0.5 λ at 0.6238 μm. This is a double pass measurement, so the WFE for a single pass is 0.25 λ. If this is scaled to λ = 2.0 μm, the WFE is approximately 0.078 λ peak to valley.

The final cryogenic issue addressed prior to integration was the survivability of the optical coatings. Witness samples were produced for the various coatings for each of the optics. These were thermally cycled to ensure survivability.

5. INITIAL IMAGE RESOLUTION RESULTS

The integration and test plan for the MWIR HSI included testing of the infinite conjugates prior to assembly into the imager. The front objective and telecentric infinite conjugate lenses were tested by evaluating the image resolution.

Figure 10: Target for Testing Front Objective (left) and Image on Microbolometer (right)

The front objective was evaluated by imaging a target illuminated with a blackbody source using the lens assembly and a room temperature microbolometer (Boeing). To create quantitative measure of resolution, a bar pattern was generated on a brushed aluminum surface. The smallest resolvable bar spacing was calculated based on the instantaneous field of view (IFOV). This is based on

$$\delta_{obj} = \frac{\delta_{pixel}}{EFL} \times d_{obj}$$

where d_{obj} is the distance between the microbolometer and the object (4 m), the EFL is the effective focal length of the lens (50 mm), and δ_{pixel} is the pixel size for the camera (51 μm). The minimum resolvable feature is 4 mm. Therefore, a series of bars was created at a spacing of 3 mm, 6 mm, and 12 mm (see Figure 10). The bars are clearly visible in the microbolometer image shown on the right. Each pixel in the image represents a pixel on the microbolometer array.

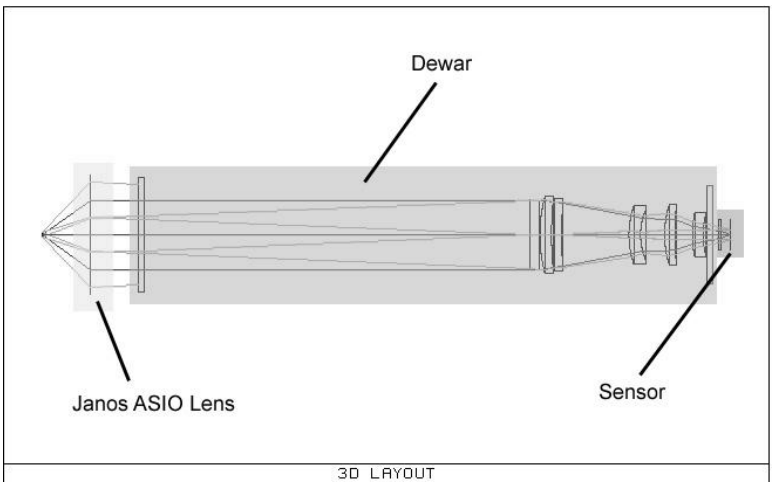

Figure 11: Configuration for Testing the Cyrogenic Telecentric Infinite Conjugate

Testing the telecentric infinite conjugate required mounting the lens inside the dewar. As such, it was not practical to image an object at a finite distance. In general, the depth of the dewar produced severe vignetting at the edge of the field. Instead, an off the shelf (Janos ASIO f = 25 mm) infinite conjugate was used outside the dewar and a telecentric imaging system was formed (see Figure 11). This system was used to form an image of a USAF Resolution target that was patterned on a ZnSe window and illuminated with a blackbody source.

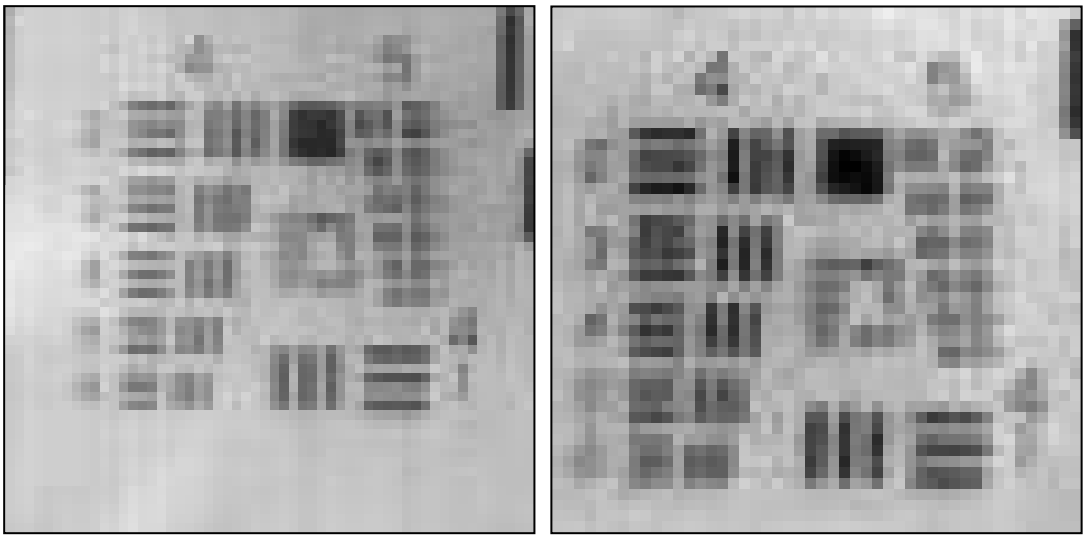

Figure 12: Center of the USAF Resolution Target Imaged by Telecentric Infinite Conjugate: Room Temperature (left) and Cryogenic Temperature (right) – Demonstrating 50 μm Resolution

Figure 12 shows the finest resolution resolved using the USAF Resolution target for both room temperature and cryogenic temperature. Group 4, Element 3 and/or Group 4/Element 4 are resolvable (25 μm resolution on the target). The combination of the telecentric lens under test and the ASIO lens produced a magnification of 2.0X. As a consequence, the image represents a resolution of 50 μm – the limit of the pixel size of the microbolometer.

6. SUMMARY

Real-time hyperspectral imaging in the MWIR is a challenging goal. We have presented our design for a system that can produce hyperspectral images from 2 μm – 5 μm. It incorporates cryogenically cooled optics for high SNR and a modest footprint and mass for portability. It will operate when the optics are at room temperature or at cryogenic temperature. Design issues specific to cryogenically cooled systems were addressed. Finally, initial imaging resolution data was discussed. This data shows that the resolution of the optics at both room temperature and cryogenic temperature is at least 50 μm.

7. REFERENCES

1. M. Dombrowski, J. Bajaj, and P. Willson, "Video-rate Visible to LWIR Hyperspectral Imaging and Image Exploitation," 31st Applied Imagery Pattern Recognition Workshop, October 2002.
2. M. Dombrowski, , P. Willson and C. LaBaw, "Performance and Application of Real-Time Hyperspectral Imaging," SPIE Imaging Spectrometry IV, Vol 3438, July 1998.
3. M. Bayar, "Lens Barrel Optomechanical Design Principles," Optical Engineering 20:181.
4. P. Yoder, Optomechanical Systems Design, Second Edition, Marcel Dekker 1992 pp 191-192.